*Progress In Electromagnetics Research C, Vol. 17, 121–130, 2010*

# HARMONICS MEASUREMENT ON ACTIVE PATCH ANTENNA USING SENSOR PATCHES

**D. Zhou**

Surrey Space Centre, University of Surrey
Guildford, GU2 7XH, UK

**R. A. Abd-Alhameed and C. H. See**

Mobile and Satellite Communications Research Centre
University of Bradford, Bradford, BD7 1DP, UK

**N. T. Ali**

Electronic Engineering, Sharjah Campus
Khalifa University of Science, Technology & Research (KUSTAR)
P. O. Box 573, Sharjah, UAE

**M. S. Bin-Melha**

Mobile and Satellite Communications Research Centre
University of Bradford, Bradford, BD7 1DP, UK

**Abstract**—Performance of the sensing patch technique for measuring the power accepted at the antenna feed port of active patch antennas has been evaluated at harmonic frequencies. A prototype antenna, including two sensors at appropriate locations, was fabricated and tested at the fundamental and two harmonic frequencies to estimate the power accepted by the antenna, including determination of the sensor calibration factor.

*Received 28 September 2010, Accepted 29 October 2010, Scheduled 8 November 2010*
Corresponding author: Dawei Zhou (d.zhou@surrey.ac.uk).

## 1. INTRODUCTION

The active integrated antenna (AIA) has been growing area of research over the recent years, due to its compact size, low weight, low cost, and multiple functionalities. An AIA can generally be considered as an active microwave circuit in which the output or input port is free space instead of conventional 50 Ω interface. In all cases, the antenna is fully (or closely) integrated with the active device to form a subsystem on the same board and can provide certain circuit functions such as resonating, duplexing, filtering as well as radiating, that describes its original role. AIAs are typically classified into three types: amplifying-type, oscillating-type and frequency-conversion-type, according to how the active device acts in the antenna [1–8].

In general, radiated power by the active integrated antenna at the targeted design frequency and its harmonics can be measured using Friis transmission equation in the anechoic chamber [9]. In addition, a simple measurement technique for measuring the power accepted by the active patch antenna, using a sensing patch feeding a network or spectrum analyzer, was first proposed in [10]. The technique eliminates many uncertainties and errors, such as cable losses, effects of the pattern, effects of nearby scatterers, and gain estimation errors, and even makes it unnecessary to operate in the far field. This technique was originally developed for the measurement of amplifying-type active patch antennas at their fundamental design frequency. It was subsequently applied to measurements on oscillating-type antennas [11].

In this paper, the possibility of using this technique to find the power accepted by the antenna at harmonic frequencies is studied. Performance of the sensing patch technique for measuring the power accepted at the antenna feed port of active patch antennas at harmonic frequencies is evaluated using an electromagnetic (EM) simulator Ansoft Designer@ [12] in terms of the current distribution. A prototype antenna, including two sensors at appropriate locations around the patch, is fabricated and tested at three designated frequencies to estimate the accepted power by the antenna, including determination of the sensor calibration factor. It is shown, based on experimental results, that the original technique can also be employed to measure the second harmonic power; measurement of the third harmonic power is also possible if another sensing patch is added in an appropriate position.

## 2. SENSOR SIMULATION AND MEASUREMENT OF HARMONICS

An inset microstrip-fed patch antenna, resonating at 2.44 GHz, was chosen for the test, since this type of antenna is convenient for the design of active oscillator antennas. The important dimensions of this antenna have been illustrated in Fig. 1. The performance of the sensing patch method at 2nd and 3rd harmonic frequencies was evaluated with this antenna. The current distribution on the patch at harmonic frequencies was first studied to find the proper position for the sensing patch. Figs. 2 and 3 show the corresponding harmonic current distributions on the patch. The position of the sensing patch is optimally set adjacent to a point of maximum voltage, which corresponds to a point of minimum current distribution on the patch. Thus the position of the sensing patch can be set next to the middle of the end edge of the patch for the 2nd harmonic and one-third of the way along one side of the patch for the 3rd harmonic. It was also found that the presence of the sensing patch has very little effect (about $\pm 0.2$ dB) on the return loss at the input port of the main patch at the fundamental operating frequency and the first two harmonics as

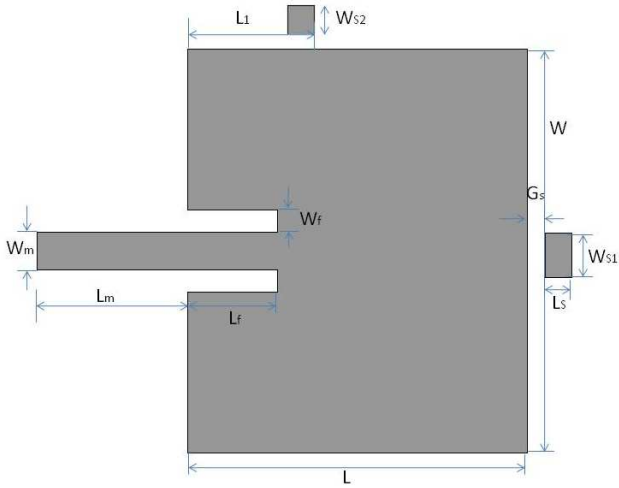


**Figure 1.** Important dimensions of the patch antenna studied in this paper ($W = 38.15$, $L = 45.96$, $L_1 = 18.32$, $W_m = 4.24$, $L_m = 17$, $W_f = 2.54$, $L_f = 10.02$, $G_s = 2$, $W_{s1} = 5$, $W_{s2} = 3$ and $L_s = 3$; all dimensions in millimetre).

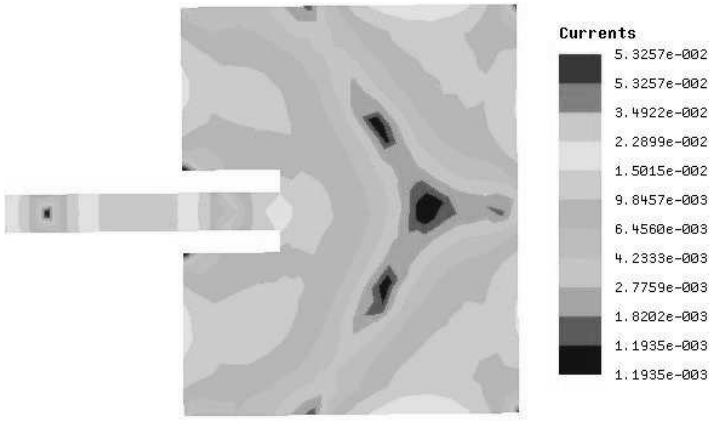


**Figure 2.** Current distribution on the patch antenna at 2nd harmonic frequency.

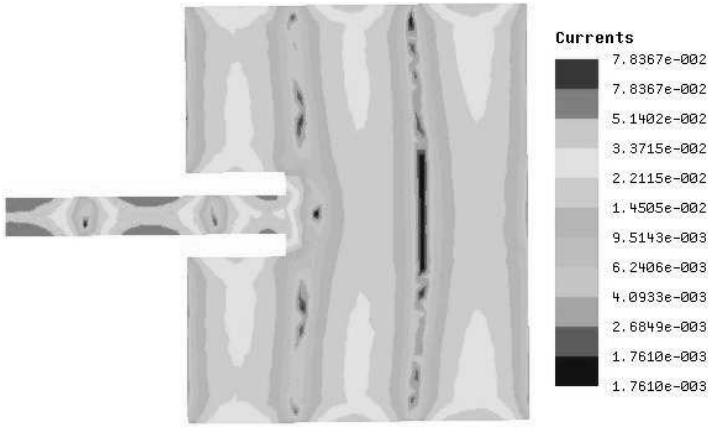


**Figure 3.** Current distribution on the patch antenna at 3rd harmonic frequency.

shown in Fig. 4.

The antenna with two sensing patches was mounted on 1.524 mm thick Duroid substrate material with relative permittivity of 2.55 and loss tangent of 0.0018. The sizes of the sensing patches used for the 2nd and 3rd harmonic frequencies were 3 mm × 5 mm and 3 mm × 3 mm, respectively. A spacing distance of 2 mm between the sensing patches and the antenna patch (see Fig. 5) was found acceptable for sufficient coupling and had no noticeable effect on the antenna input return loss. It has to be noted that the sensing patch at the 2nd harmonic has the

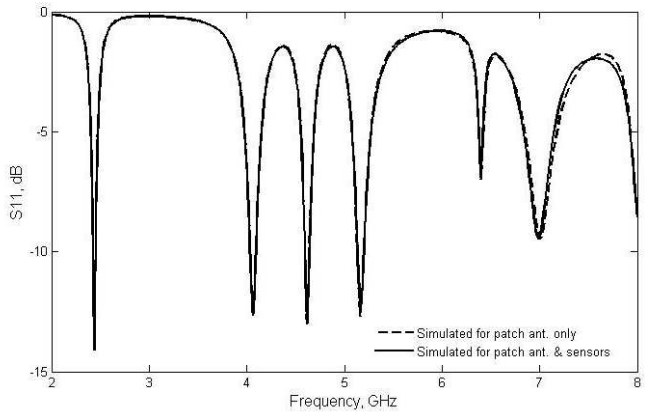


**Figure 4.** Simulated antenna return loss with and without the sensor patch.

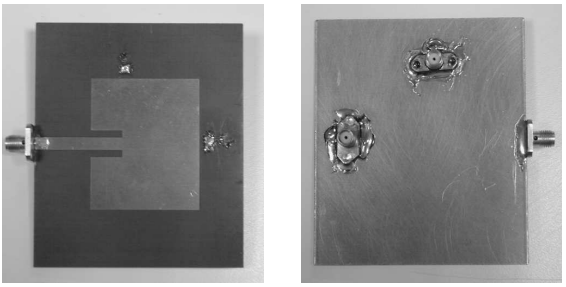

**Figure 5.** Fabricated antenna showing sensor locations: (left) Top view, (right) Underside.

same location as at the fundamental. The sensing patch was connected to ground via a 50-ohm chip resistor. The inclusion of the 50-ohm resistor creates a relatively well-matched source for the attached cable. A 50-ohm coaxial probe was mounted at the rear of the circuit board and connected to the resistor load: This fed the sensor output to a traceably-calibrated network analyzer.

The sensing patch for the 2nd harmonic was first tested. According to the work presented in [10], the performance of the sensing patch for harmonics can be evaluated using the calibration factor $|S'_{21}|$, which relates the sensor's output power to the power accepted by the radiator from RF circuitry (e.g., a RF power amplifier or oscillator),

as follows:

$$\left|S'_{21}\right|^2 = \left|S_{21}\right|^2 / \left(1 - \left|S_{11}^2\right|\right) \tag{1}$$

where $[S] = \begin{bmatrix} S_{11} & S_{12} \\ S_{21} & S_{22} \end{bmatrix}$.

The scattering parameters $[S]$ in Eq. (1) were obtained by measuring two-port $S$-parameters between the antenna input feed line and the sensor's output from 2 GHz to 8 GHz using a traceably-calibrated network analyzer (HP 8510C). The variations of the measured $[S]$'s extended over the fundamental frequency and the first two harmonics are presented in Fig. 6; the corresponding calibration factor from the measured antenna data was computed using Eq. (1). The measured return loss and computed calibration factors are presented in Table 1 at 2.44, 4.88, and 7.32 GHz, respectively.

In order to evaluate the sensor's calibration factor for harmonics, a 0 dBm RF signal was injected into the main patch from a sweep oscillator HP 8350B at the fundamental and harmonic frequencies. The

**Table 1.** 2nd harmonic sensor measurement results for the fundamental and harmonics.

| Freq (GHz) | $S_{11}$ (dB) | $\lvert S'_{21}\rvert^2$ (dB) | $L_{\text{cable}}$ (dB) | $P_{\text{reading}}$ (dBm) | $P_{\text{accepted}}$ (dBm) | $P'_{\text{accepted}}$ (dBm) |
|---|---|---|---|---|---|---|
| 2.44 | −24.86 | −23.20 | 1.33 | −25.33 | −0.0144 | −0.8 |
| 4.88 | −1.75 | −20.42 | 2.67 | −28.5 | −4.796 | −5.412 |
| 7.32 | −4.241 | −23.45 | 4 | −27 | −2.052 | 0.45 |

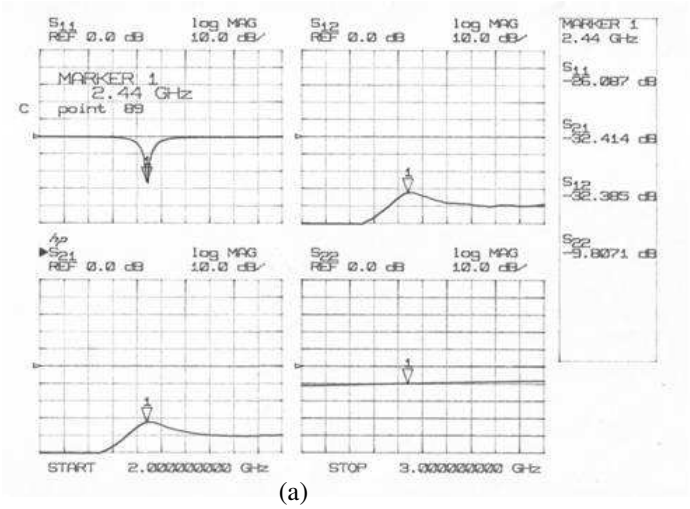


(a)

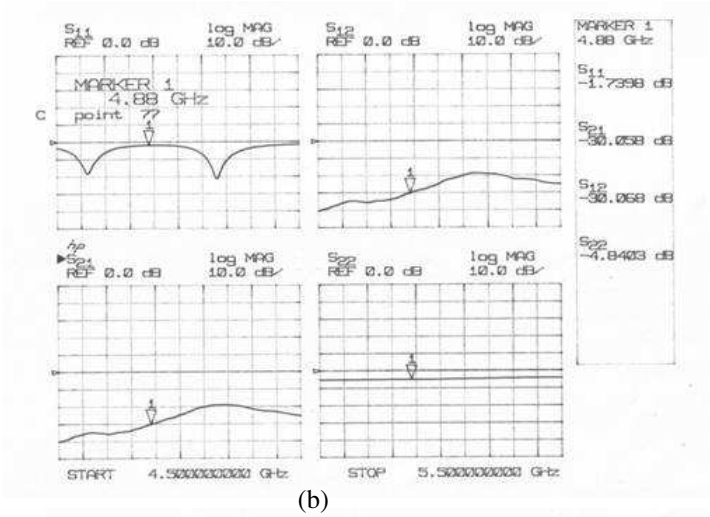


**Figure 6.** Measured two-port $S$-parameters between the antenna input port and the sensor's output port at, (a) fundamental frequency, (b) 2nd harmonic frequency, (c) 3rd harmonic frequency.

measurement setup is illustrated in Fig. 7. The Return Loss (R.L.) of the antenna tested was optimized at its fundamental frequency into an impedance of $50\,\Omega$, as shown in Table 1. However, at harmonic frequencies, the input impedance of the antenna was greatly different from $50\,\Omega$. Thus, the power accepted by the antenna ($P_{\text{accepted}}$) is

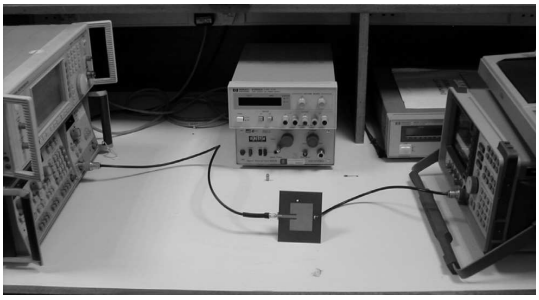

**Figure 7.** Photograph of measurement setup in this study.

given by:

$$P_{\text{accepted}} = P_{\text{incident}} \left(1 - |\Gamma|^2\right) \tag{2}$$

where $\Gamma$ is the reflection coefficient at the input of the antenna and $|\Gamma|^2 = P_{\text{reflected}}/P_{\text{incident}}$. $P_{\text{reflected}}$ is the power reflected at the antenna input, and $P_{\text{incident}}$ is the power outgoing from the signal generator (in this case, $P_{\text{incident}} = 0\,\text{dBm}$ at all frequencies). The power from the sensor's output ($P_{\text{reading}}$) was observed using a spectrum analyzer (HP 8563A). Care was taken to find the loss in the cable ($L_{\text{cable}}$) before measuring the output power from the sensor. The estimated power accepted by the antenna ($P'_{\text{accepted}}$) can be found as:

$$P'_{\text{accepted}} = P_{\text{reading}} - \left|S'_{21}\right|^2 - L_{\text{cable}} \tag{3}$$

A summary of measured parameters for the 2nd harmonic sensor is presented in Table 1. The technique shows that the power accepted by the antenna at the fundamental and 2nd harmonic frequencies can be achieved using the same sensing patch. As can be seen from Table 1, the accuracy of this technique is around 0.7 dB (i.e., the maximum difference between the $P_{\text{accepted}}$ and $P'_{\text{accepted}}$ at the fundamental and 2nd harmonic). It should be noted that the power accepted at the 3rd harmonic frequency varies greatly in the measurement and this is because the sensor at this position is weakly coupled to the maximum voltage of the 3rd harmonic.

Similarly, for the 3rd harmonic sensor, the same process was used as with the 2nd harmonic sensor. A summary of measured parameters for the 3rd harmonic sensor is presented in Table 2 at the intended frequencies. It is shown that the technique is still valid within 1 dB accuracy for 3rd harmonic power measurement. In addition, this sensor can also be applied for the 2nd harmonic power measurement, with very good accuracy. This is because the current distribution at

**Table 2.** 3rd harmonic sensor measurement results for the fundamental and harmonics.

| Freq (GHz) | $S_{11}$ (dB) | $\lvert S'_{21}\rvert^2$ (dB) | $L_{\text{cable}}$ (dB) | $P_{\text{reading}}$ (dBm) | $P_{\text{accepted}}$ (dBm) | $P'_{\text{accepted}}$ (dBm) |
|---|---|---|---|---|---|---|
| 2.44 | −26.09 | −32.403 | 1.33 | −33 | −0.0109 | 0.733 |
| 4.88 | −1.74 | −25.25 | 2.6 | −33 | −4.814 | −5.155 |
| 7.32 | −4.19 | −23.59 | 4 | −30.67 | −2.084 | −3.08 |

the 2nd harmonic frequency near to the location of the 3rd harmonic sensor is close to minimum, and this can be easily seen from Fig. 3. It is notable that the power accepted at the fundamental frequency varies greatly in the measurements. In addition, care should be taken on means of improving the port impedance matching at the sensor patch port in order to eliminate measurement errors and improve measurement accuracy at fundamental and harmonic levels using this proposed technique. This challenging problem including the antenna operation over a wide frequency band is left to future work.

## 3. CONCLUSION

The measurement of the power accepted by a microstrip patch antenna, using the sensing patch measurement technique, has been demonstrated at both fundamental and first two harmonic frequencies. The results of the present work were exhibited to be acceptable and agreed with direct measurements. The proposed technique was shown to achieve 0.7 dB and 1 dB relative accuracy for the 2nd and 3rd harmonic measurements respectively.

## REFERENCES

1. Kaya, A. and S. Comlekci, "The design and performance analysis of integrated amplifier patch antenna," *Microwave and Optical Technology Letters*, Vol. 50, No. 10, 2732–2736, October 2008.
2. Kim, H. and Y. J. Yoon, "Wideband design of the fully integrated transmitter front-end with high power-added efficiency," *IEEE Transactions on Microwave Theory and Techniques*, Vol. 55, No. 5, 916–924, May 2007.
3. Chou, G.-J. and C.-K. C. Tzuang, "Oscillator-type active-integrated antenna: The leaky-mode approach," *IEEE Transactions on Microwave Theory and Techniques*, Vol. 44, No. 12, 2265–2272, December 1996.

4. Choi, D.-H. and S.-O. Park, "Active integrated antenna using T-shaped microstrip-line-fed slot antenna," *Microwave and Optical Technology Letters*, Vol. 46, No. 6, 538–540, September 2005.
5. Cha, K., S. Kawasaki, and T. Itoh, "Transponder using self-oscillating mixer and active antenna," *IEEE MTT-S Int. Microwave Symp. Digest*, 425–428, 1994.
6. Montiel, C. M., L. Fan, and K. Chang, "A novel active antenna with self-mixing and wideband varactor-tuning capabilities for communication and vehicle identification applications," *IEEE Transactions on Microwave Theory and Techniques*, Vol. 44, No. 12, Part 2, 2421–2430, 1996.
7. Bilotti, F., F. Urbani, and L. Vegni, "Design of an active integrated antenna for a PCMCIA card," *Progress In Electromagnetics Research*, Vol. 61, 253–270, 2006.
8. Yang, S., Q.-Z. Liu, J. Yuan, and S.-G. Zhou, "Fast and optimal design of a k-band transmit-receive active antenna array," *Progress In Electromagnetics Research B*, Vol. 9, 281–299, 2008.
9. Balanis, C. A., *Antenna Theory: Analysis and Design*, 3rd edition, 94–96, John Wiley & Sons Inc., 2005.
10. Elkhazmi, E. A., N. J. McEwan, and N. T. Ali, "A power and efficiency measurement technique for active patch antennas," *IEEE Transactions on Microwave Theory and Techniques*, Vol. 48, No. 5, 868–870, May 2000.
11. Abd-Alhameed, R. A., P. S. Excell, and E. Elkhazmi, "Design of integrated-oscillator active microstrip antenna for 2.45 GHz," *XXVIIth General Assembly of URSI*, Paper No. 1181, Maastricht, August 2002.
12. Ansoft Designer, Version 1.0, Ansoft Corporation, USA.